

#### RESEARCH ARTICLE

# Dynamics of turbulent flow over mobile dune

Pradyumna Kumar Behera<sup>1</sup>, Vishal Deshpande<sup>2</sup> and Bimlesh Kumar<sup>1</sup>

**Corresponding author:** Bimlesh Kumar; Email: bimk@iitg.ac.in

Received: 4 June 2025; Revised: 7 October 2025; Accepted: 27 October 2025

Keywords: higher-order structure functions; mobile bed forms; non-Gaussian characteristics; PDFs; scour depth

#### **Abstract**

The present study reveals the turbulence dynamics and morphological adjustments of mobile dune-shaped bedforms in an alluvial stream. Results demonstrate acceleration of flow over the dune crest enhancing streamwise velocity, while the initial and the lee side sections of the dune experience flow circulation. The near-bed regions of the initial and lee sections experience peak Reynolds shear stress, marking zones of higher momentum exchange and active sediment entrainment. Turbulence is dominated by streamwise fluctuations, with spanwise and vertical components reinforcing lateral mixing and particle suspension. Octant analysis indicates that sweep events dominate in the near-bed regions of the initial, crest and lee sections of the dune, driving bedform migration and intensifying scour development on the lee side. Probability distribution functions highlight strong non-Gaussian behaviour and intermittency at crest and lee sections, linked to vortex shedding and flow separation. Higher-order structure functions further confirm the presence of intense turbulent bursts in the near-bed region, underscoring the role of coherent structures in driving sediment motion. Morphological analysis shows progressive scour development at the lee side and downstream crest erosion, resulting in continuous dune migration. These findings advance understanding of turbulence—morphology interactions and their control on sediment transport in alluvial channels.

# **Impact Statement**

- Comprehensive analysis of streamwise flow velocity, Reynolds shear stress (RSS) and turbulent intensity
  patterns over different sections of the mobile bedforms.
- 2. The study provides insight into the flow's randomness and chaotic nature by analysing the probability distribution function (p.d.f.) of velocity fluctuations and RSS.
- Detailed investigations on the flow field's higher-order structure function to understand the turbulence's multi-scale nature.
- 4. Assessment of bedform growth and migration with time.

# 1. Introduction

Sediment transport in alluvial channels can alter both the flow dynamics and the morphological characteristics of the channel, potentially leading to the development of bed features. Bedforms, which may range from ripples to dunes depending on the flow velocity, are dynamic topographic features that naturally develop on the beds of alluvial channels due to sediment movement driven by flowing water. The volume and rate of sediment transport are strongly influenced by flow velocity, turbulence and the

<sup>&</sup>lt;sup>1</sup>Department of Civil Engineering, Indian Institute of Technology Guwahati, Guwahati, Assam, India

<sup>&</sup>lt;sup>2</sup>Department of Civil and Environmental Engineering, Indian Institute of Technology Patna, Patna, Bihar, India

coherent structures generated within the channel due to obstructions such as bedforms (Huai *et al.*, 2020; Wang *et al.*, 2023; Mishra *et al.*, 2024; Mahon *et al.*, 2024).

The size of sediments entrained and transported can vary from fine particles, such as silt and sand, to coarse materials, including gravel, depending primarily on the prevailing flow conditions. Rapid changes in hydraulic conditions can significantly disrupt the sediment transport equilibrium, leading to substantial morphological changes in alluvial streams over short periods (Kleinhans, 2001, 2002; Carling *et al.*, 2005; Tayfur and Singh, 2006, 2007). As a result, understanding how dunes and other bedforms interact with flow dynamics is crucial for modelling sediment transport in fluvial systems (ASCE Task Force, 2002; Li *et al.*, 2024).

Research has shown that coherent turbulent structures are key in initiating sediment movement in natural channels (Best, 1992; Raudkivi, 1997). This sediment mobilisation often results in the transition from flatbeds to more complex two-dimensional and three-dimensional bedforms (Raudkivi and Witte, 1990; Robert and Uhlman, 2001; Venditti *et al.*, 2005; Zomer and Hoitink, 2024; Das *et al.*, 2024). More recent findings indicated that turbulent flow events, especially those producing strong horseshoe vortices, can intensify scour processes and accelerate sediment erosion in alluvial streams (Ikani *et al.*, 2023; Bauri *et al.*, 2024).

Field observations in braided river systems have identified dunes as a dominant form of bedform deposit, particularly in sandy riverbeds (Best *et al.*, 2003; Bridge, 2003). These dunes are characteristically asymmetrical, featuring a gently inclined upstream slope (stoss side), where the flow velocity gradually increases, and a steep downstream slope (lee side), which experiences a sudden decrease in elevation, accompanied by flow deceleration due to flow separation and recirculation zones. Both experimental investigations and numerical modelling (Bridge, 2003; Lyn and Altinakar, 2002; Yue et al., 2006; Dimas *et al.*, 2008; Xie *et al.*, 2014) have consistently shown a wake zone with circulating eddies and a shear layer that divides the recirculating flow from the main flow.

Understanding turbulence characteristics in alluvial channels is crucial for predicting sediment transport, bedform development and channel morphology. Due to the highly stochastic and nonlinear nature of turbulence, traditional deterministic models are often inadequate (Lu & Willmarth, 1973; Nakagawa & Nezu, 1977). Therefore, various researchers have extensively applied probability distribution functions (p.d.f.s) and structure functions to capture the statistical behaviour of turbulent flow parameters and coherent structures in the flow field (Grass, 1971; Cellino & Graf, 2000). P.d.f.s offer a statistical framework to describe these fluctuations at a given point or over a specific spatial domain. In mobile-bed alluvial systems, analysing the p.d.f.s associated with the fluctuating components can provide valuable insights into the frequency and intensity of turbulence, which are directly linked to sediment entrainment and transport (Nezu *et al.*, 1993).

Previous experimental studies by Nezu (1977) and Antonia *et al.* (1995) showed that streamwise and vertical velocity fluctuations in open-channel flows deviate from normality in the near-bed region. Skewed or heavy-tailed p.d.f.s have been more successful in representing the velocity distributions in these regions (Raupach 1981). These p.d.f.s are particularly effective in capturing the intermittent, high-intensity turbulent events responsible for sediment detachment. Similarly, Reynolds shear stress (RSS), which governs the momentum exchange in turbulent flows, exhibits strong temporal and spatial variability. The p.d.f.s of RSS in the near-bed region of an alluvial stream are observed to be non-Gaussian and often display a positive skew reflecting the dominance of high-magnitude turbulent bursts that enhance sediment entrainment, near-bed mixing and momentum exchange, which play a critical role in driving erosion and bedform evolution (McLean *et al.*, 1994; Shvidchenko & Pender, 2001).

Recent numerical simulations using Reynolds-averaged Navier–Stokes (RANS), large eddy simulation (LES) and direct numerical simulation (DNS) methods have used p.d.f.s to validate turbulence models and to evaluate the probabilistic behaviour of subgrid-scale stresses and eddies (Yue *et al.*, 2006). P.d.f.s derived from these models help to tune turbulence closure models and improve predictive capabilities under complex boundary conditions like seepage, sediment motion or mobile bed deformation. Similarly, among the various tools developed to quantify turbulent fluctuations, structure functions of higher-order moments have proven instrumental in exploring the scaling behaviour and intermittency

within turbulent boundary layers. These functions capture the statistical moments of velocity increments over varying spatial or temporal separations, thus enabling insights into the energy cascade and anomalous scaling behaviour in the inertial range (Sreenivasan *et al.*, 1997).

Classical turbulence theory postulates a universal scaling for the second-order structure function in the inertial subrange, assuming local isotropy and self-similarity (Frisch & Kolmogorov, 1995). However, subsequent experimental and numerical investigations have consistently revealed deviations from this linear scaling at higher orders, indicating the presence of intermittent, localised, intense bursts of velocity fluctuations that simple dimensional arguments cannot capture (Anselmet *et al.*, 1984; Benzi *et al.*, 1996). These deviations have motivated the development of refined models, including extended self-similarity (ESS) and multifractal formulations, to better account for the observed non-Gaussianity and scale-dependent behaviour (Parisi & Frisch, 1985).

In the flow field above dune bed features, these high-order moments offer critical information about the momentum transfer and flow-bed interactions, especially under modified conditions such as sediment mobility (Marusic *et al.*, 2013). Recent studies have extended the analysis of these moments into the logarithmic region of turbulent boundary layers, demonstrating that the 2*p*th moment of velocity fluctuations raised to the power 1/*p* follows a generalised logarithmic law, emphasising the universality and structural consistency of turbulent flows at high Reynolds numbers (Pathikonda & Christensen, 2017). Thus, integrating p.d.f.-based approaches and structure–function in analysing the flow field in the alluvial channel has proven advantageous in capturing the stochastic nature of entrainment and deposition (Einstein, 1950).

While the analytical tools such as p.d.f.s, turbulence intensities and higher-order structure functions have been extensively employed in previous literature to analyse the turbulence patterns in alluvial channels, their application to mobile dune-shaped bedforms and how they influence sediment transport behaviour along the dune has remained unexplored. Previous studies have examined turbulence statistics over fixed dunes or have treated morphological evolution separately from turbulence analysis. The present study addresses this gap by integrating turbulence statistics with continuous measurements of dune morphology. This study aims to find out the direct linkage between the turbulent intermittency, coherent structures and non-Gaussian velocity fluctuations to dune crest erosion, scour formation and downstream migration. Thus, the study provides new physical insights into how turbulence characteristics govern sediment entrainment and transport from different sections of the dune during the transition from an initially mobile bedform towards a quasi-equilibrium state.

# 2. Experimental set-up and methodology

The experiments were carried out in a hydraulics flume with dimensions of 20 m (length)  $\times 1 \text{ m}$  (width)  $\times 0.72 \text{ m}$  (depth). The flume was installed with a longitudinal slope of approximately 0.0025, determined using a Total Station. A comprehensive description of the flume design and set-up is provided by Behera *et al.* (2024). A schematic representation showing the flume side elevation and main structural components is illustrated in Figure 1.

River sand was used as the bed material for flume preparation. The sand had a median grain diameter  $(D_{50})$  of 1.1 mm and was distributed uniformly across a mesh above the underlying pressure chamber. The geometric standard deviation of the sediment particle was found to be 1.03, indicating that the sediment was well-graded and met uniformity standards as outlined by Marsh *et al.* (2004). The dry repose angle of the sand was measured at 31.154°, reflecting its natural stability on the flume bed. The resulting Shields parameter  $(\theta)$  for the present study was found to be 0.193, whereas the critical Shields parameter  $(\theta_c)$  was estimated to be 0.0322. Thus, the ratio of the Shields parameter with respect to the critical Shields parameter  $\theta$ / $\theta$ <sub>c</sub>  $\approx$  6, indicating the flow substantially exceeds the threshold for particle motion, which can result in continuous bedload transport.

The sand particles were used to create dune-shaped bedforms. These dune-shaped bedforms were modelled based on the empirical relationships proposed by Van Rijn (1984), which related the bedform geometry to sediment size, flow depth and transport conditions depending on the flow regime.

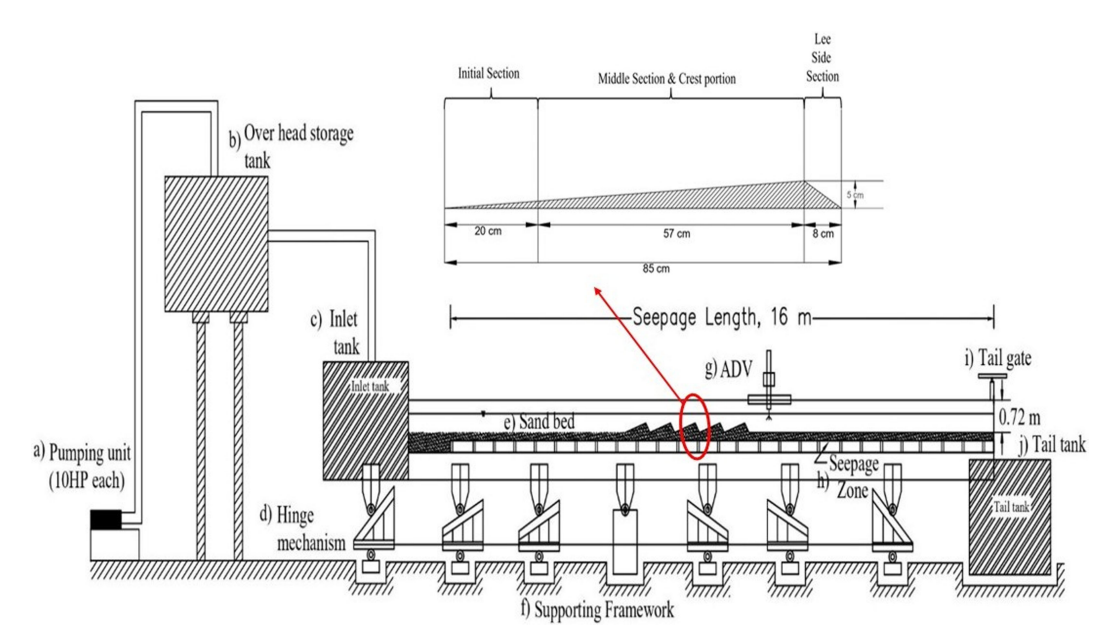


*Figure 1.* Schematic diagram illustrating the experimental flume (side view) and locations of instantaneous velocity measurement over the dune.

To replicate these bedforms within the flume, metal sheets matching the target profile of the bedform were temporarily fixed along the sidewalls. The sand was packed between the sheets to form the structure. Once compacted, the sheets were carefully removed, leaving behind well-defined dunes.

The constructed bedforms occupied a 5 m section between 10 m and 15 m downstream of the flume inlet to minimise disturbances from inlet and outlet effects. Flow measurements focused on the third dune, which is centrally located within this section. The flow depth was consistently maintained at 14 cm for the experimental studies. A 0.5 m wide rectangular notch installed at the tail end of the flume was used for discharge measurement (Deshpande and Kumar, 2016). The flow rate was established at  $0.042 \text{ m}^3 \text{ s}^{-1}$  and the average streamwise velocity was  $0.30 \text{ m s}^{-1}$ . Calculated dimensionless numbers indicated the flow regime under turbulent subcritical flow, with a Reynolds number of 41 860 and a Froude number of 0.218.

Each dune had a width of 1.0 m and a total length of 0.85 m, consisting of a gently sloping stoss side (0.77 m) and a steep lee side (0.08 m). The dune crest rose 5 cm above the base at 77 cm along the profile, then sharply dropped to the bed level by 85 cm. Van Rijn (1984) developed the equation for calculating the bedform dimensions based on transport stage parameter, depth of flow and particle size diameter. From the sediment size and flow specification in the present study, dimensionless ratios are evaluated to check and justify whether the dune dimensions are within the range specified by Van Rijn (1984). The calculation of the dimensionless ratios is provided in Table 1.

Five such dunes were constructed between the 10 and 15 m positions along the flume to ensure flow development before and after the test section. Instantaneous velocity measurements over the central dune profile were captured using a four-beam, down-looking acoustic Doppler velocimeter (ADV). Data were collected at ten vertical positions along the third dune. Systematic instantaneous velocity measurements were carried out at 10 different sections along the length of the dune as shown in Figure 2. The 10 sections consist of four initial sections (0–30 cm), the four middle sections (40–70 cm), the crest portion (77 cm) and the lee section (83 cm). This comprehensive measurement approach allowed us to capture the complete flow field evolution over the central line of the dune profile. However, the results shown in the present study are limited to a few critical sections where distinct transitions in flow behaviour were observed, such as at the initial section, the middle section, the crest and the lee side section, where the flow pattern changes. These sections were selected because they best illustrate the shift from acceleration over the stoss side to flow separation and recirculation on the lee side. Presenting results at every

Flow

Table	1	Dimer	ision	1000	ratio
IUIILE		Dimer	เงเบทเ	PAL	<i>rance</i>

Dimensionless ratio	Evaluated value	Typical dune range (as specified by Van Rijn (1984))	Remarks
Relative dune	0.357	0.05-0.4	Reasonable
depth $(H/h)$			
Length-to-height	17	10-20	Acceptable
ratio $(L/H)$			
Length and	773	500-2000	Fits Van Rijn's
particle-based			empirical data
scaling $(L/D_{50})$			
Height and	45	10–50	Reasonable
particle-based			
scaling $(H/D_{50})$			
Froude number	0.256	< 1	Subcritical flow
Reynolds number	41 860	Re > 2000	Turbulent flow

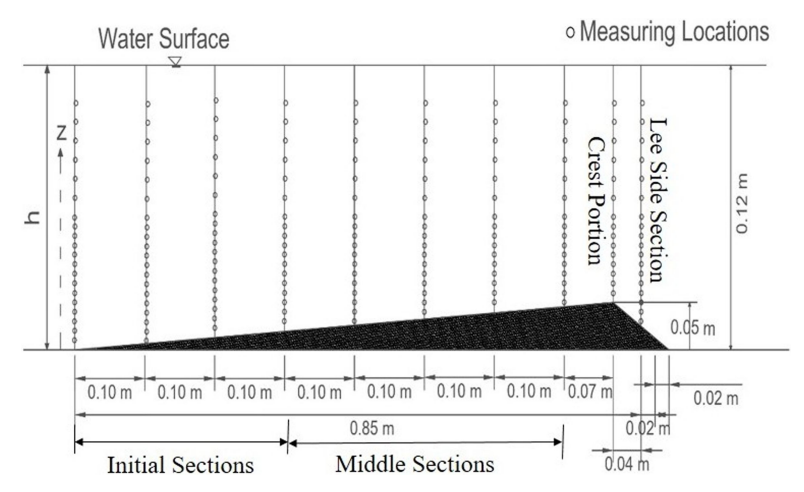


Figure 2. Instantaneous velocity measurements over the dune.

measured section would have added redundancy and complexity, making interpretation less clear (see Figure 2).

The ADV sampling frequency for instantaneous velocity measurement was set to 100 Hz for the instrument. The instrument set-up, calibration and data collection methodology follow the procedures detailed by Behera *et al.* (2024). Post-processing of velocity data included the removal of signal spikes using the acceleration threshold technique described by Goring and Nikora (2002), which identifies and corrects anomalous values in the velocity time series. The acceleration threshold method is a detection and replacement technique used for removing spikes from the instantaneous velocity data collected by the ADV. It operates in two phases: one for negative accelerations and the second for positive accelerations. In each phase, numerous passes through the data are made until all data points conform to the acceleration criterion and the magnitude threshold.

Before conducting the actual experimental runs, the reliability and precision of velocity measurements were verified through uncertainty analysis. Ten repeated trials were conducted with the ADV positioned 3 mm above the bed surface. Each trial included 15 signal samples, comprising 12 000 samples collected for two minutes at 100 Hz. The resulting standard deviations and associated uncertainties for the longitudinal, lateral and vertical velocity components, and their respective turbulent fluctuations are presented by Behera *et al.* (2025).

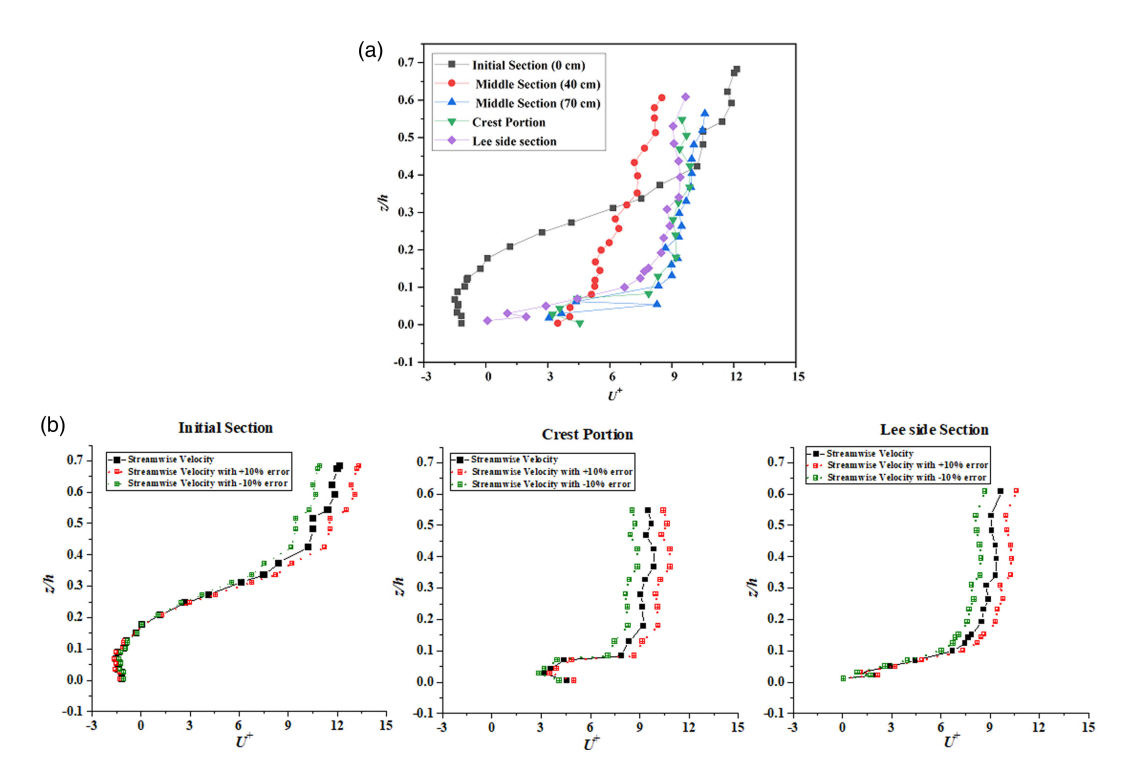


Figure 3. Variation of non-dimensional (a) streamwise velocity at some critical sections of the dune and (b) streamwise velocity with error plot.

# 3. Results

# 3.1. Time-averaged streamwise velocity

The non-dimensional time-averaged velocity  $(U^+)$  in the direction of flow can be estimated using

$$U^{+} = \frac{\frac{1}{n} \sum_{i=1}^{n} U_{i}}{U_{+}},\tag{1}$$

where n defines the number of samples recorded at individual measurement locations and  $U_i$  depicts the instantaneous velocity measured in the longitudinal direction of flow. To compare the flow patterns, the instantaneous velocity readings of all the sections along the length of the dune are normalised with a constant value of shear velocity  $U_*$  (= 2.97 cm s<sup>-1</sup>), estimated at the dune's crest portion. The value of shear velocity obtained at the crest portion is estimated using the turbulent kinetic energy method in the near-bed region (z/h < 0.25) (Taye and Kumar, 2021). Figure 3 illustrates the variation of non-dimensional streamwise velocity at some critical sections along the length of the mobile dune.

At the initial section, the velocity profile shows a steady and continuous increase with depth towards the surface of the water. The negative value of streamwise velocity in the near-bed region at the dune's initial sections confirms the flow circulation due to a strong wake effect from an upstream dune. In the middle sections (40 and 70 cm) on the stoss side of the dune, the streamwise velocity increases more rapidly in the region z/h < 0.4, confirming enhanced shear and acceleration of flow as it ascends the dune slope. The velocity profile at 77 cm shows a similar trend, with maximum velocity observed in this zone, reflecting further flow adjustment and momentum gain.

At the lee side section of the dune, the streamwise flow velocity is lower as compared with the velocity at the crest section, indicating a recirculation or wake zone resulting from flow separation at the dune crest and the subsequent reattachment process downstream. While this zone exhibits typical post-crest flow behaviour, an important observation is that the streamwise velocity in the near-bed region on the

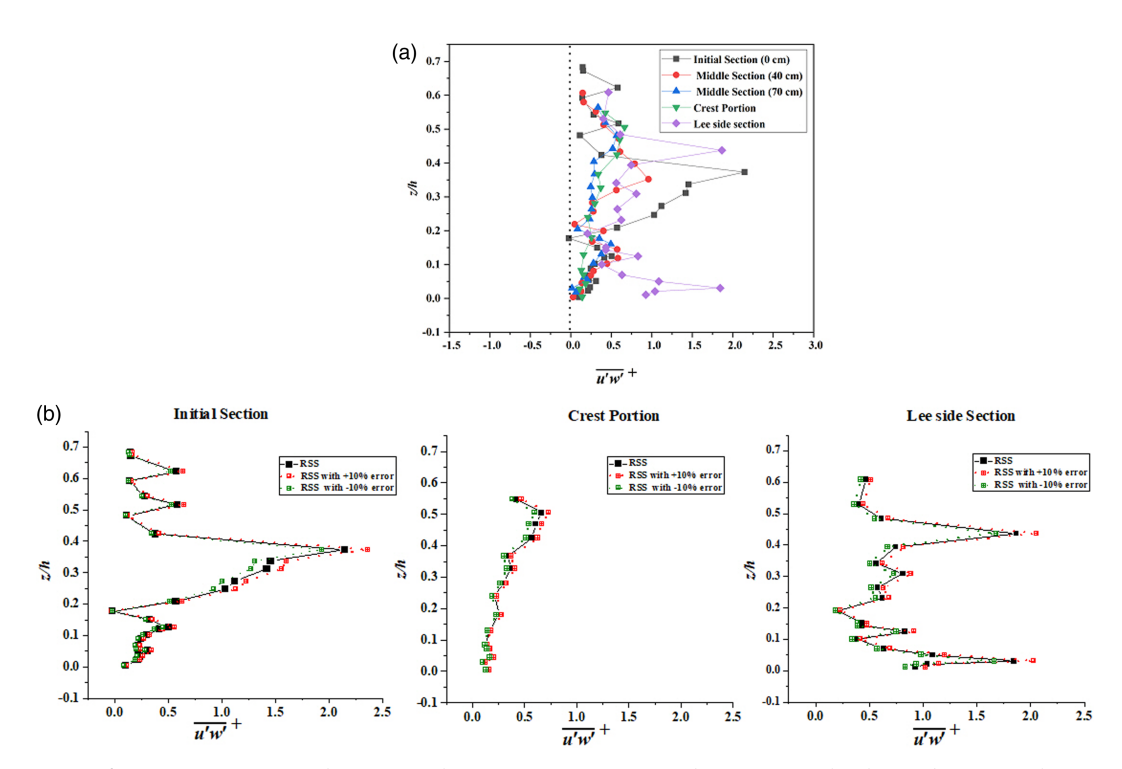


*Figure 4.* Variation of non-dimensional (a) RSS at some critical sections of the dune, (b) RSS with error plot.

lee side of the considered dune is higher than at the initial section. This suggests that the wake generated by the preceding dune (influencing the initial section) is stronger than the wake formed at the lee side of the current dune.

# 3.2. Reynolds shear stress

A higher Reynolds shear stress (RSS) value at a given location in the flow field depicts greater momentum exchange within the flow. Studies have revealed that bed features in the flow field cause higher Reynolds stress patterns, leading to higher momentum exchange (Bernard and Handler, 1990). The plot of non-dimensional RSS against the normalised vertical position (z/h) at various sections along the dune reveals the spatial variability in turbulent momentum flux, as shown in Figure 4. The momentum flux influences sediment entrainment, transport and deposition, providing insights into bedform evolution (Järvelä, 2005; Yang & Choi, 2009; Huai *et al.*, 2019). The non-dimensional RSS ( $\tau_{uw}$ ) in the flow can be presented by

$$\overline{u'w'}^{+} = \frac{-\rho_w \overline{u'w'}}{\rho_w \left(U_*^2\right)} \tag{2}$$

where u' and w' are the fluctuating components associated with the flow in streamwise and vertical directions, respectively, and  $\rho_w$  is the density of water.

At the initial section (0 cm) and the lee-side section (77 cm) of the dune, the RSS is observed to be relatively high. The magnitude of the RSS is maximum at 0.2 < z/h < 0.4 and in the near-bed region. The observation indicates intense turbulent mixing and strong momentum exchange between the flow layers in the initial sections. Physically, this elevated turbulence near the bed enhances the ability of the flow to entrain and transport sediment particles, contributing to bedform initiation and mobility. The

shear stress distribution suggests a well-developed turbulent boundary layer that actively interacts with the mobile bed, potentially initiating sediment.

The patterns of RSS at the middle sections (40 and 70 cm) exhibit moderate values, with peaks more concentrated in the near-bed regions. This trend implies that the flow is adjusting to the evolving bedform geometry. As the flow traverses the dune, sediment particles already in motion may continue to be transported, but the capacity for fresh sediment entrainment diminishes slightly due to reduced shear intensities towards the end sections of the stoss side of the dune. This could represent a zone of transitional sediment transport, where the morphology begins to stabilise and the flow gradually approaches an equilibrium condition with the bedform.

RSS at the crest portion of the dune is featured by a sharp peak near the water's surface. In the near-bed region, the trend exhibits the lowest values, with a flatter and less structured profile and a flattened trend. This value suggests that sediment motion at the crest portion is not as profound as in the region of the lee-side sections or the initial sections. However, localised erosion at the crest portion may occur, reshaping the crest and contributing to the dune's downstream migration.

# 3.3. Turbulent intensities

Turbulent intensity determines the contribution of fluctuating velocity components in the streamwise, spanwise and vertical flow directions. A higher turbulent intensity corresponds to higher turbulence in the flow field. Non-dimensional turbulent intensities in the streamwise  $(\sigma_u^+)$ , spanwise  $(\sigma_v^+)$  and vertical  $(\sigma_w^+)$  directions are given by (3)–(5), respectively:

$$\sigma_u^{+} = \frac{\sqrt{\frac{\sum_{i=1}^{n} (Ui - U)^2}{n-1}}}{U_*},\tag{3}$$

$$\sigma_{v}^{+} = \frac{\sqrt{\frac{\sum_{i=1}^{n} (Vi - V)^{2}}{n-1}}}{U_{*}},$$
(4)

$$\sigma_{w}^{+} = \frac{\sqrt{\frac{\sum_{i=1}^{n} (Wi - W)^{2}}{n-1}}}{U_{+}},$$
(5)

where u', v' and w' are the fluctuating components associated with the flow in streamwise, lateral and vertical directions, respectively.

Figures 5(a)–5(c) show the distribution of non-dimensional turbulence intensities in the streamwise, spanwise and vertical directions, respectively.

Among the three components of turbulent intensity, the streamwise turbulence intensity is most pronounced in the flow as compared with the turbulent intensity in the vertical and spanwise directions. At the initial section (0 cm) and middle section (40 cm) of the dune, high values are observed in the region of 0.25 < z/h < 0.45. In the region near the crest portion (70 cm) and at the crest portion sections (77 cm), the elevated turbulence intensities in the near-bed region indicate strong fluctuations in the streamwise velocity component, a direct consequence of flow acceleration over the rising bedform. The lee-side section shows significantly higher streamwise turbulence intensity, reflecting a region of intense mixing due to the formation of a scour hole. This spatial variability illustrates how the dune's shape governs the distribution of shear stress and, consequently, the erosion and deposition zones.

Similar to the streamwise velocity pattern, at the dune's initial section (0 cm), the magnitude of lateral turbulent intensity is higher in the region of 0.25 < z/h < 0.45. It exhibits moderate values across the middle sections, indicating lateral instabilities induced by the three-dimensional structure of the bedform. These spanwise fluctuations contribute to the redistribution of sediment perpendicular to the main flow direction, facilitating the maintenance of the dune's transverse geometry and enhancing mixing. However, spanwise turbulence increases in the near-bed region of the crest portion and the lee-side

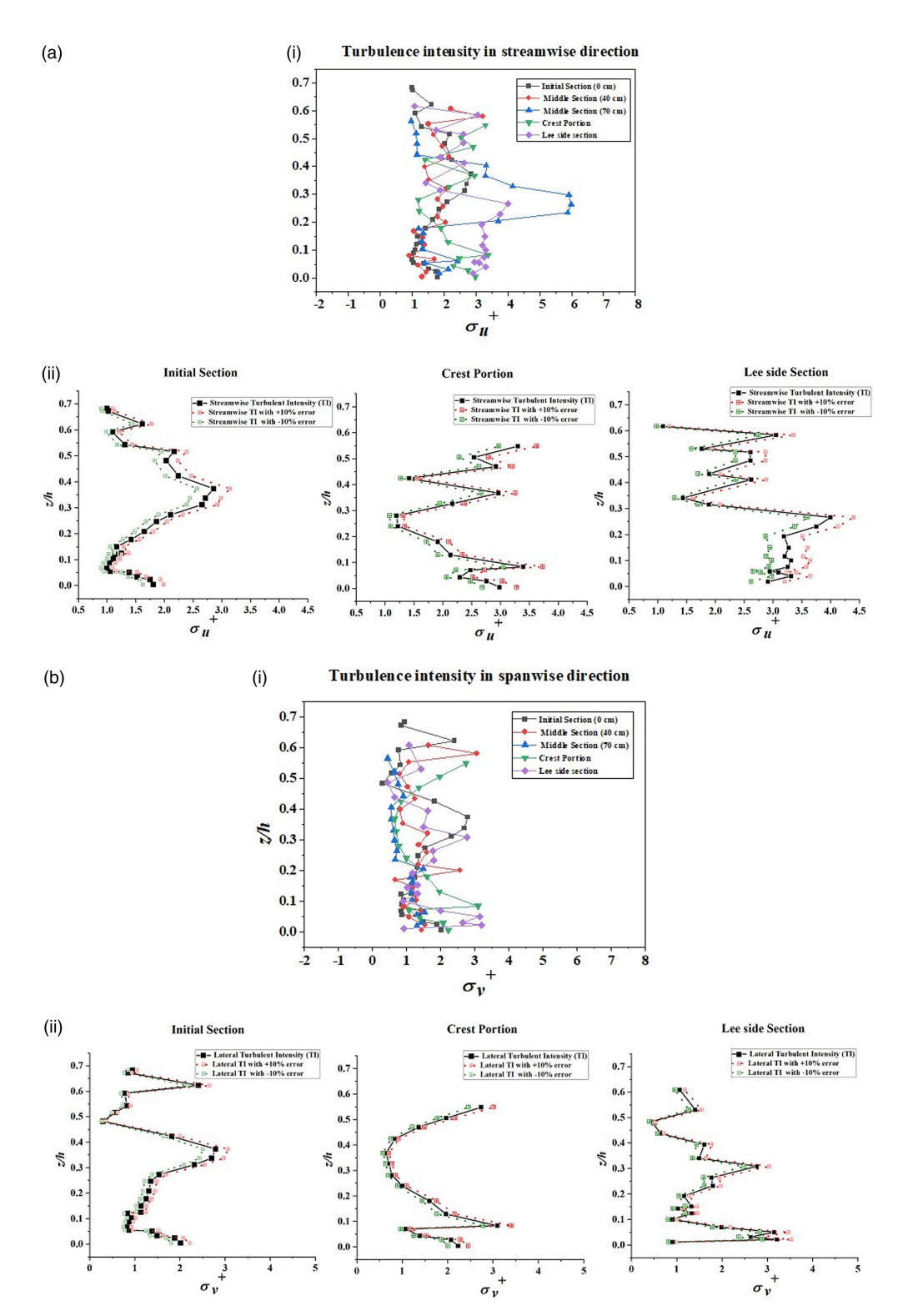
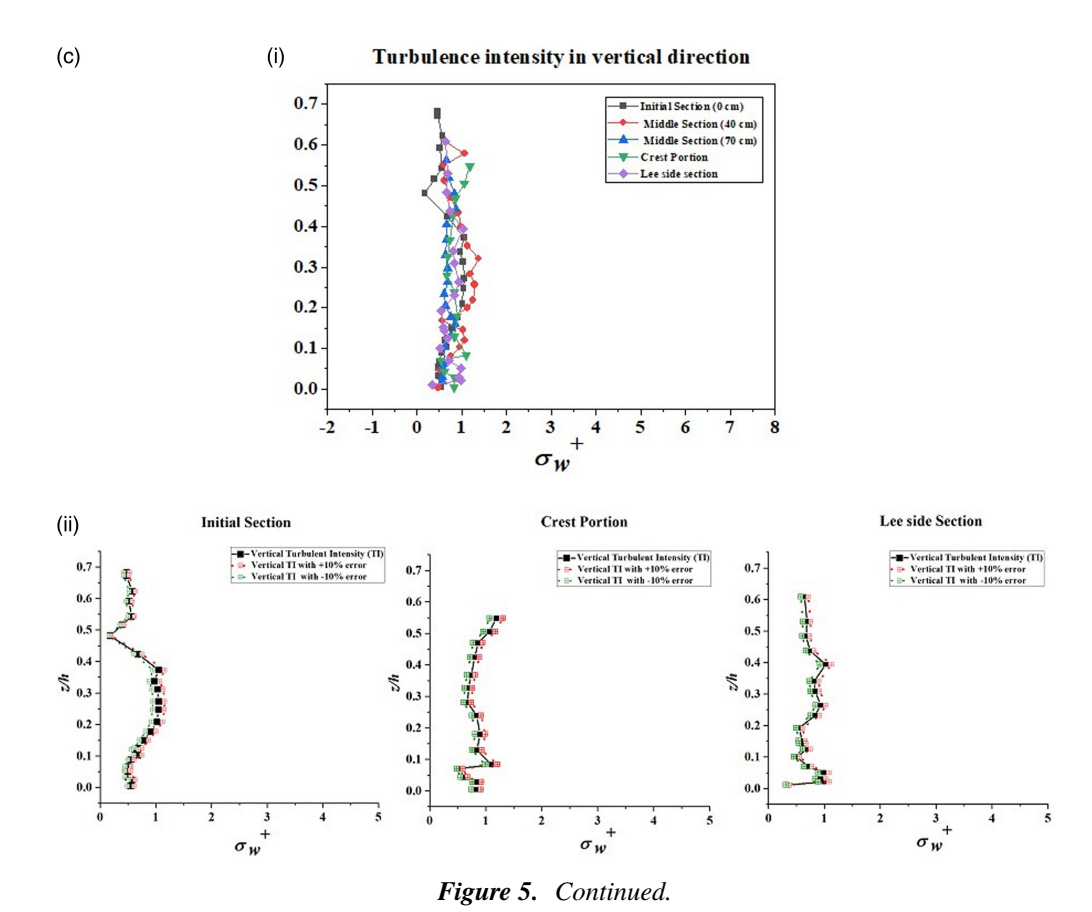


Figure 5. (a) Variation of non-dimensional (i) streamwise turbulent intensity at some critical sections of the dune, (ii) streamwise turbulent intensity with error plot. (b) Variation of non-dimensional (i) spanwise turbulent intensity at some critical sections of the dune, (ii) spanwise turbulent intensity with error plot. (c) Variation of non-dimensional (i) vertical turbulent intensity at some critical sections of the dune, (ii) vertical turbulent intensity with error plot. https://doi.org/10.1017/flo.2025.10035 Published online by Cambridge University Press



section, reinforcing higher energy dissipation in the flow due to the development of scour holes on the lee-side section of the dune.

The magnitude of vertical turbulence intensity is the lowest among the three turbulent intensities. Across all sections, vertical turbulence remains relatively uniform, showing only minor variations among the different bedform positions. This suggests a more consistent vertical momentum exchange throughout the flow field. However, slightly higher vertical turbulence in the near-bed region of the crest portion and the lee-side sections indicates localised upward bursts and turbulent events capable of lifting particles.

# 3.4. Octant analysis of bursting events

Octant analysis quantifies different bursting events associated with the turbulent characteristics of flow into eight bursting events as follows.

- 1. Class I-A, Internal outward interaction (u' > 0, v' > 0, w' > 0).
- 2. Class II-A, Internal ejection (u' < 0, v' < 0, w' > 0).
- 3. Class III-A, Internal inward interaction (u' < 0, v' < 0, w' < 0).
- 4. Class IV-A, Internal sweep (u' > 0, v' > 0, w' < 0).
- 5. Class I-B, External outward interaction (u' > 0, v' < 0, w' > 0).
- 6. Class II-B, External ejection (u' < 0, v' > 0, w' > 0).
- 7. Class III-B, External inward interaction (u' < 0, v' > 0, w' < 0).
- 8. Class IV-B, External sweep (u' > 0, v' < 0, w' < 0).

Flow

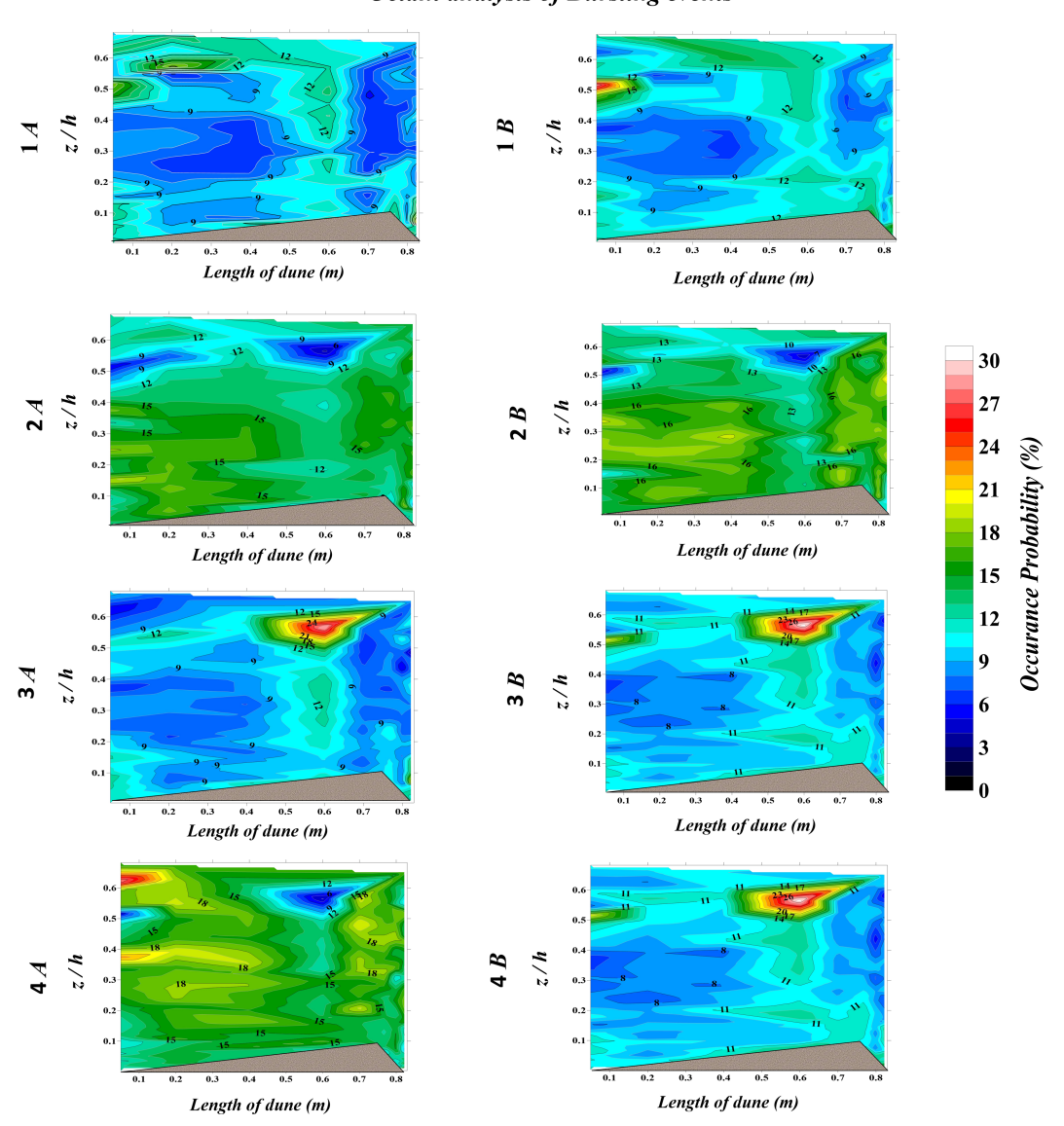


Figure 6. Occurrence probability of bursting events along the dune.

The occurrence probability of each event can be defined as (Keshavarzi and Gheisi, 2006)

$$P_k = \frac{n_k}{N},\tag{6}$$

where  $N = \sum_{k=1}^{8} n_k$ ,  $k = 1, 2, 3, 4 \dots, 8$ ..

Here,  $P_k$  is the occurrence probability of each event,  $n_k$  is the number of events in each class and N is the total number of bursting events. Figure 6 represents the occurrence probability of different bursting events across the dune.

The probabilities of occurrence of internal outward interaction (Class I-A) and external outward interaction (Class I-B) events are low to moderate probability ( $\sim$ 6%–12%) across the dune length. The probability of occurrence of I-A has slightly higher intensity in the near-bed region and upstream dune face, while I-B shows localised stronger events near the crest. The findings suggest that outward interactions are less dominant, contributing minimally to strong Reynolds stress generation. However, the

probabilities of occurrence of both inward and outward ejection (Class II-A and Class II-B) events are higher. The inward and outward ejection (Class II-A and Class II-B) events dominate at the crest portion and lee-side sections of the dune and stoss side. The study also confirms that ejection events (upward motion of low-momentum fluid) are major contributors to turbulence in the wake zone located at the lee side of the dune.

The internal and external inward interaction (Class III-A, Class III-B) shows lower probabilities of occurrence throughout the flow field along the length of the dune. Although some localised peaks in the occurrence of internal inward interaction (Class III-A) can be observed in mid-depth regions and external inward interaction (Class III-B) can be observed near the crest location, the dominance of this event is less. However, the probabilities of occurrence of an internal sweep event (Class IV-A) are very strong near the bed and stoss side, showing strong downward momentum transport in the near region at the initial section and the lee-side section of the dune, which will enhance sediment transport behaviour. Further, a very strong dominance external sweep event (Class IV-B) can be observed at the dune crest, which suggests dune crest movement along the flow direction leading to overall bedform migration. The results confirm that sweeps (downward rush of high-momentum fluid) dominate in the near-bed region of the initial section, crest portion and lee-side section of the dune, confirming strong turbulence production, which is crucial for sediment entrainment.

# 3.5. Probability distribution functions

P.d.f.s in turbulence represent the likelihood of observing a specific value of a fluctuating quantity over time, which helps quantify turbulence's randomness and chaotic nature. Mathematically, for a random variable x, the p.d.f. f(x) satisfies

$$P(x_1 < x < x_2) = \int_{x_1}^{x_2} f(x) \, \mathrm{d}x,\tag{7}$$

where *x* represents the velocity fluctuations or turbulent shear stress. Details about the probability distribution function of fluctuating components and RSS, along with the equation to evaluate it, are provided by Sharma and Kumar (2017) and Gurugubelli *et al.* (2025).

# 3.5.1. Probability function of fluctuating component

Figure 7 depicts the p.d.f. of streamwise velocity fluctuations ( $P_u$ ) plotted against the normalised velocity fluctuation ( $\hat{u}$ ) at some critical sections along a dune. At the initial section (0 cm), the experimental data are relatively well-aligned with the theoretical curve, with a peak value of approximately 0.35. However, there is some scatter in the tails, especially in the positive range. These results suggest that although extreme velocity fluctuation events characterise this section, the flow is adjusting to the presence of the bedform.

The experimental data in the middle sections of the dune start to deviate more from the theoretical prediction, with an observable right-skewness in the distribution. This asymmetry signifies stronger turbulent interactions and the amplification of flow instabilities due to a steepening slope and streamline convergence, which elevate the likelihood of high-magnitude streamwise velocity fluctuations. The agreement between theoretical and experimental data further deteriorates at the crest portion. The experimental curve is broader and flatter, indicating increased turbulence intensity and a higher probability of positive and negative velocity fluctuations.

At the lee-side section, where flow separation and reattachment dominate, the experimental p.d.f. closely follows the theoretical prediction near the peak, but some spread persists in the tails. This pattern suggests that although the mean flow becomes more symmetric, the region still experiences intermittent turbulent structures, such as vortices and eddies, contributing to deviations from idealised distributions.

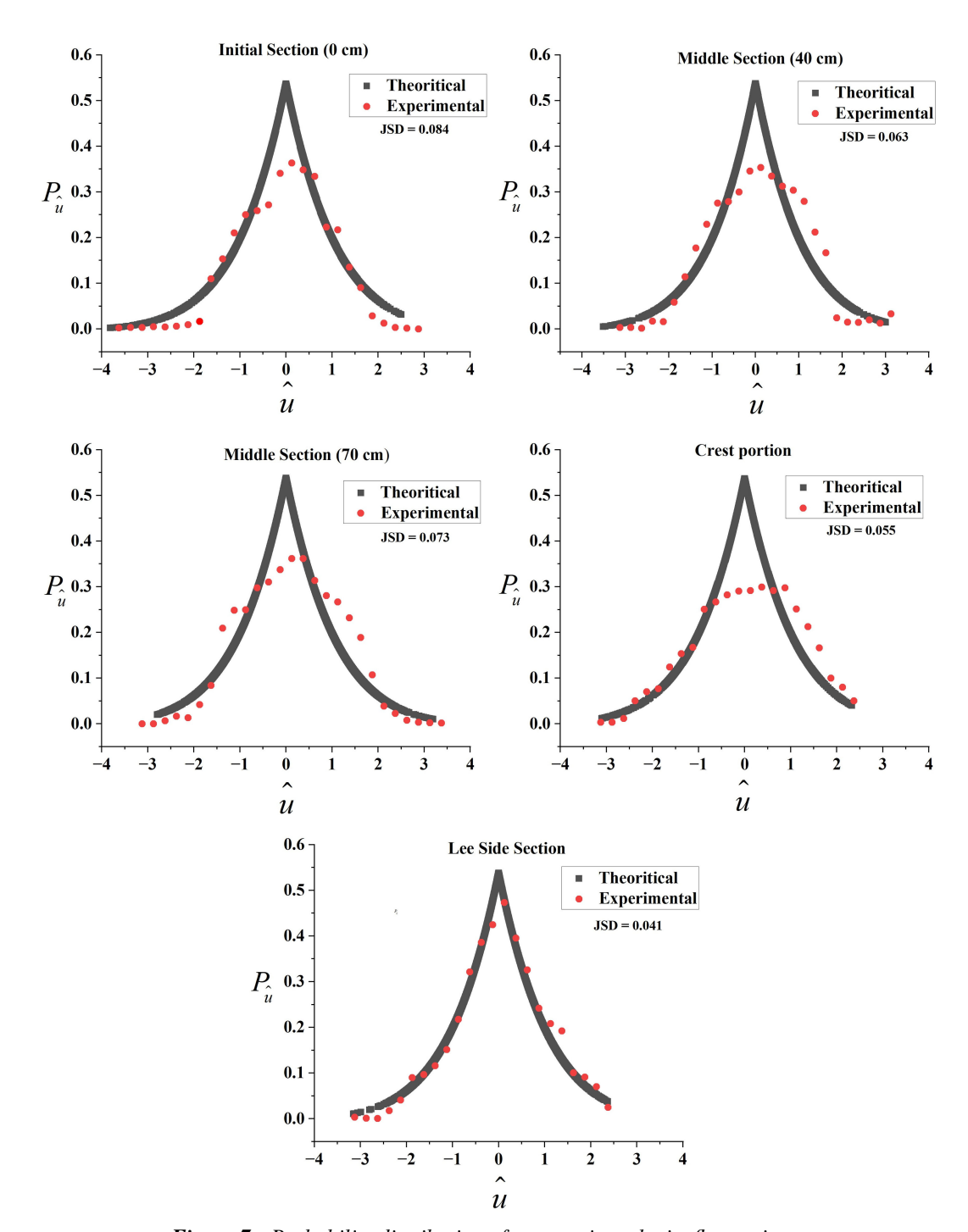


Figure 7. Probability distribution of streamwise velocity fluctuations.

The p.d.f. of lateral velocity fluctuations  $(P_{\nu})$  against the normalised lateral velocity fluctuation  $(\hat{v})$  across different sections of the dune profile is shown in Figure 8.

The dune's initial section (0 cm) is characterised by a symmetric distribution about the mean, which aligns fairly well with the theoretical curve. The close match indicates less disturbed lateral flow in this upstream region. Lateral velocity fluctuations are minimal here, showing weak cross-stream turbulent

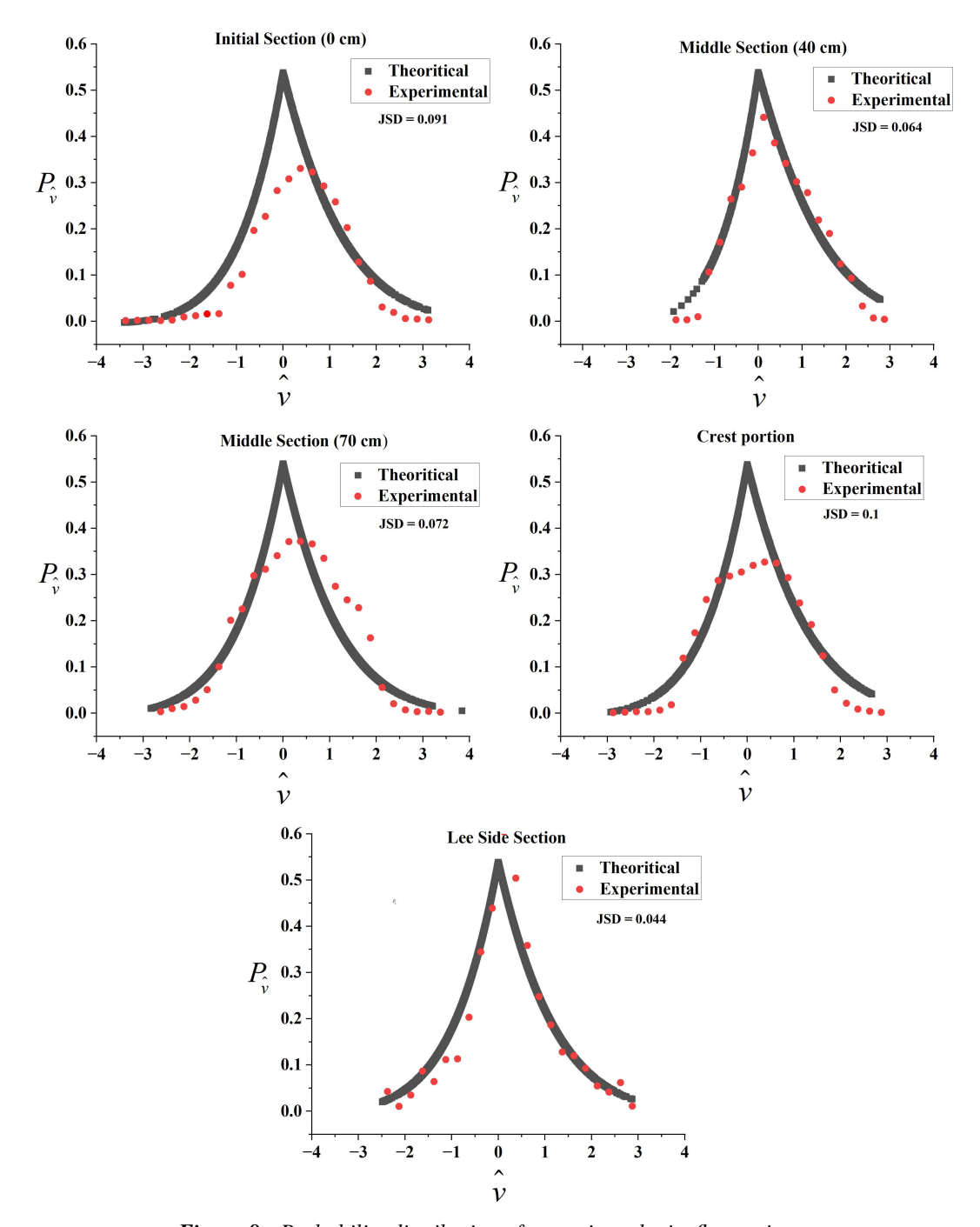


Figure 8. Probability distribution of spanwise velocity fluctuations.

activity. However, in the middle sections, the experimental data diverge slightly from the theoretical distribution, particularly in the positive fluctuation range. Evidence of a subtle increase in asymmetry indicates enhanced lateral movement due to the evolving boundary layer and interaction with the dune slope. Turbulence begins to develop more strongly, influencing the lateral component of velocity due to turbulent mixing and lateral transport, influenced by pressure gradients and flow convergence on the stoss side of the dune.

Similarly, the asymmetry at the crest portion widens further and becomes flatter than the theoretical distribution, indicating high turbulence intensity in the lateral direction. The enhanced lateral fluctuations here are physically significant, as they suggest the possible formation of lateral eddies and swirling motions, which can affect sediment suspension and redistribution. The experimental p.d.f. regains better agreement with the theoretical curve at the lee-side section, especially near the centre. The reduction in fluctuation intensity suggests a restabilisation of the flow in the lateral direction. Although residual turbulence remains from upstream interactions, the flow in the lateral direction becomes relatively more symmetric and less chaotic, which is reflected in the closer match to the theoretical p.d.f.

Figure 9 represents the distributions of the p.d.f. of vertical velocity fluctuations  $(P_w)$  against the normalised vertical velocity fluctuation  $(\hat{w})$  at some critical sections over a dune-shaped bedform.

The theoretical distributions generally exhibit a sharply peaked shape centred at zero, resembling a Laplace or exponential type distribution, indicating the assumption of symmetric and less variable vertical motions in the model. However, the experimental data deviate from the theoretical trend, especially in the middle and downstream sections, showing broader tails and occasional skewness. The experimental values deviate towards the positive side at the dune's initial and lee-side sections, suggesting asymmetric vertical velocity. The experimental p.d.f. shows broad tails, underscoring the turbulent and chaotic flow in these regions due to vortex shedding, which can enhance the sediment's vertical motion and initiate sediment transport.

However, in the middle sections of the dune, the experimental distribution becomes more symmetric with the theoretical curve, reflecting reduced vertical motions caused by the influence of the upstream dune slope. The spread of the patterns slightly narrows, indicating a partial recovery of flow stability in these regions. The crest region displays the most significant deviations between experimental and theoretical curves. The experimental p.d.f. is markedly wider, revealing strong vertical fluctuations and coherent turbulent structures.

### 3.5.2. Probability function of RSS

Figure 10 presents comparative plots of the probability density function of Reynolds shear stress  $(P_{\tau})$  against normalised shear stress  $(\hat{\tau})$  at some critical sections of the dune. It was observed that at different sections along the dune-shaped bedform, the theoretical distribution exhibits a sharp peak at  $\hat{\tau}=0$ , indicating the dominance of low-magnitude shear stress events, which is commonly observed over the alluvial bedform. However, the experimental data show varying degrees of agreement with the theoretical distribution depending on the position along the dune profile.

At the initial (0 cm) and the lee-side sections of the dune, the plot of experimental distribution function aligns well with the theoretical curve on the negative side of  $\hat{\tau}$ , but shows noticeable deviation on the positive side, suggesting asymmetries in shear stress behaviour. These dune sections display the most significant deviation between theoretical and experimental results in the positive range, representing significant flow separation and recirculation zones. The findings suggest that turbulence is highly anisotropic and disorganised due to vortex shedding. The wide scatter in experimental values indicates an abundance of energetic turbulent structures that simplified theoretical models do not capture well.

However, at the middle sections (40 and 70 cm), the correlation between experimental and theoretical distributions improves, particularly near the peak and left tail, though some divergence is still visible on the positive side. This improvement indicates the progressive development of shear layers along the stoss side of the dune as the flow accelerates along the dune and becomes more turbulent. The theoretical and experimental curves remain similar at the dune's crest, but the experimental data again show considerable spread on the positive side, signifying the onset of flow separation and strong shear layer formation.

### 3.5.3. Jensen-Shannon divergence

The Jensen–Shannon divergence (JSD) is a statistical tool used to measure the similarity between two probability distributions. In turbulence flow, JSD is applied to analyse the differences between p.d.f.s of

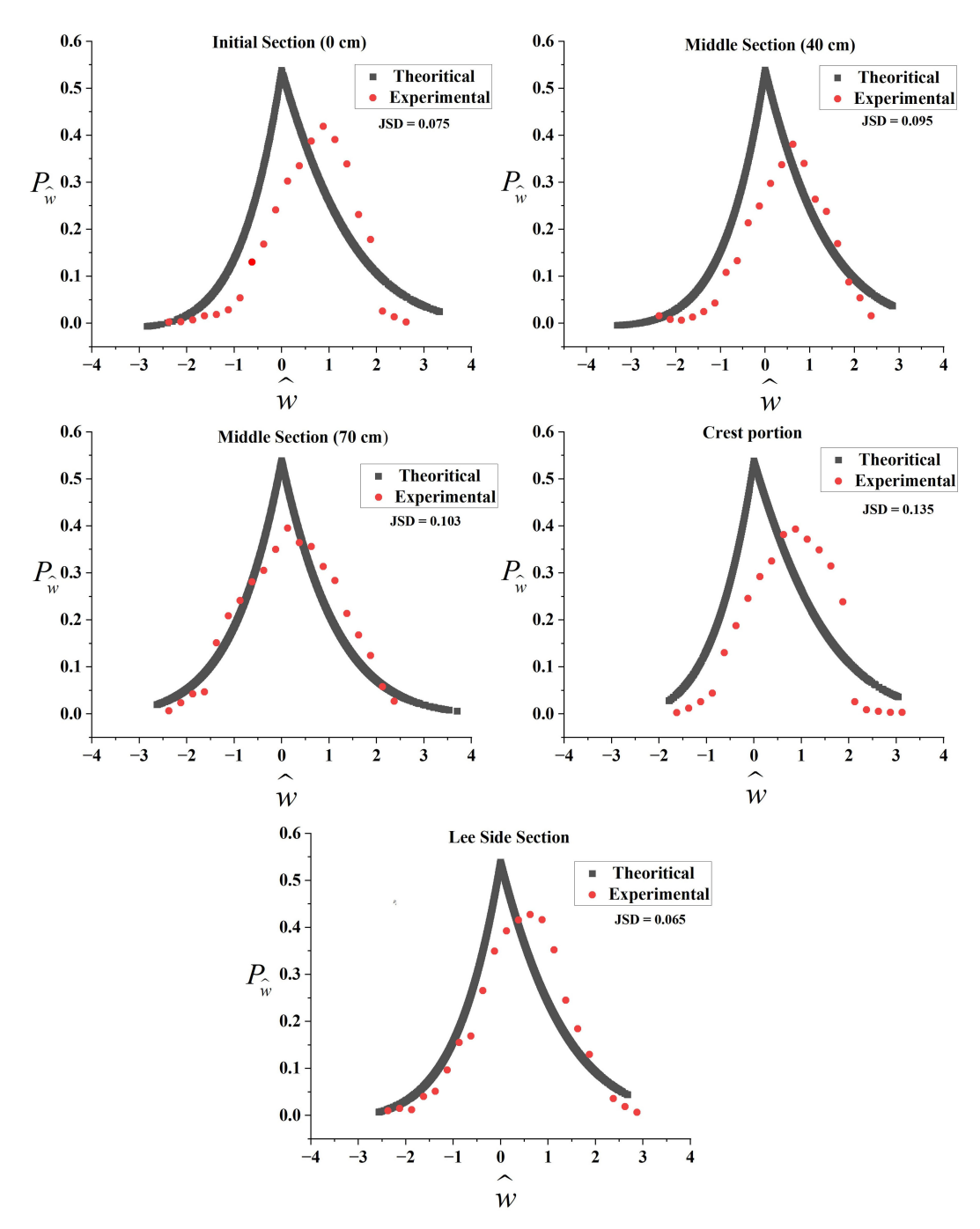


*Figure 9.* Probability distribution of vertical velocity fluctuations.

turbulence intensities between the theoretical and experimental data. It quantifies how much the turbulent characteristics deviate from a reference data set. A lower JSD value indicates that the p.d.f. of the experimental data set is more similar to the theoretical data set, while a higher value suggests greater divergence and complexity in the turbulent behaviour.

At the initial section, the probability distribution of turbulence intensity in the streamwise and spanwise directions has equal JSD values, while the probability distribution of vertical turbulence intensity

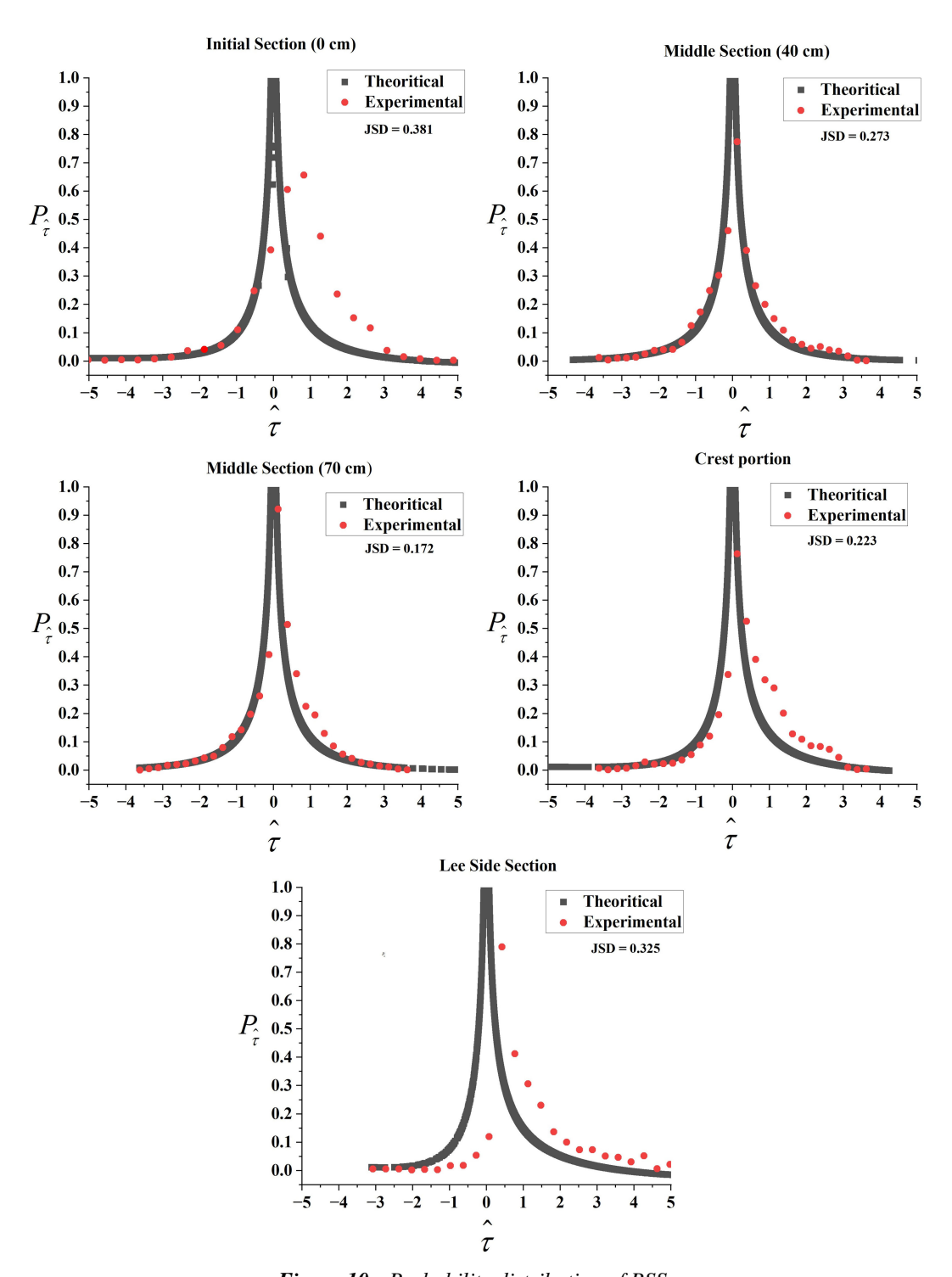


Figure 10. Probability distribution of RSS.

has a slightly lower value. The probability distribution of RSS has a JSD value of 0.375. This suggests that the flow at the initial section has a certain level of intensity and complexity. At the middle section, the JSD values for the probability distribution of streamwise and lateral turbulence intensity decrease to 0.065–0.075, indicating reduced divergence in horizontal turbulence. Contradictorily, the probability distribution of streamwise and lateral turbulence intensity increases between the range of approximately 0.095–0.105, indicating a greater influence of vertical turbulence at these sections. The JSD value for RSS also drops between 0.173 and 0.275, suggesting a more stabilised or uniform turbulence structure in the middle portion compared with the dune's initial section.

The JSD values for the probability distribution of streamwise turbulence intensity obtained at the crest portion of the dune decrease to 0.055, while lateral and vertical turbulence increase to  $\sim 0.13$ . This reflects a more asymmetrical turbulence structure with increased lateral and vertical activity prevailing at the crest portion of the dune. The slight rise in JSD value of RSS to 0.225 provides evidence of localised disturbances or transitions in the flow behaviour. However, at the lee-side section of the dune, the JSD values for the probability distribution of turbulence intensity in all directions decrease. Despite the decrease in individual turbulence intensity divergences, the divergence of RSS increases significantly to 0.325, indicating the presence of sporadic or intermittent turbulent bursts. Such elevated divergence is a direct outcome of non-Gaussian events like ejections, sweeps and vortex shedding, which occur intermittently in dune flows.

# 3.6. Higher-order structure functions

In a turbulent flow field, higher-order structure functions are statistical tools used to quantify the differences in velocity across varying spatial scales. They are critical to understanding the multi-scale nature of turbulence and provide a robust framework for characterising the strength and scale of intermittent events.

The *n*th-order structure function can be defined as

$$S_n(r) = \langle |\delta_u(r)|^n \rangle = \langle |u(x+r) - u(x)|^n \rangle, \tag{8}$$

where u(x) is the velocity at position x,  $\delta_u(r)$  is the velocity increment over distance r and n is the order of the moment. While second-order structure functions ( $S_2(r)$ ) relate to the energy spectrum, higher-order structure functions (n > 3) provide information on intermittency and non-Gaussian features of turbulence, especially in the small-scale dissipative range. Figure 11 presents the variation of the higher-order velocity fluctuation in the streamwise direction with the non-dimensional flow depth ( $z^+$ ) across different flow sections over a dune-shaped mobile bedform. Here,  $z^+ = (zu_*)/v$  is the non-dimensional distance from the bed surface of the dune.

Higher-order structure functions reveal the evolving nature of turbulent bursts, coherent structures and energy transfer mechanisms influenced by bedform topography. A general pattern is observed where the magnitude of the structure–function increases with higher orders of 2p, at all the sections. These patterns indicate a stronger contribution from intermittent turbulent events and extreme velocity fluctuations. At the initial section (0 cm), the structure–function values are relatively modest across all orders, reflecting a less developed turbulent field. However, in the near-bed region of the initial section, the magnitudes are observed to be on the higher side, suggesting extreme velocity fluctuations due to flow circulation. Similar to the initial section, in the middle section on the stoss side of the dune, an increase in the magnitude of the structure functions was observed in the near-bed region. This implies a stronger turbulent interaction, likely caused by flow acceleration and increased shear stress as the flow climbs the stoss side of the dune. At the 70 cm section, the structure–function values continue to rise, particularly towards the surface of the flow, indicating enhanced turbulence and intermittency near the surface of the water rather than in the near-bed region at these locations.

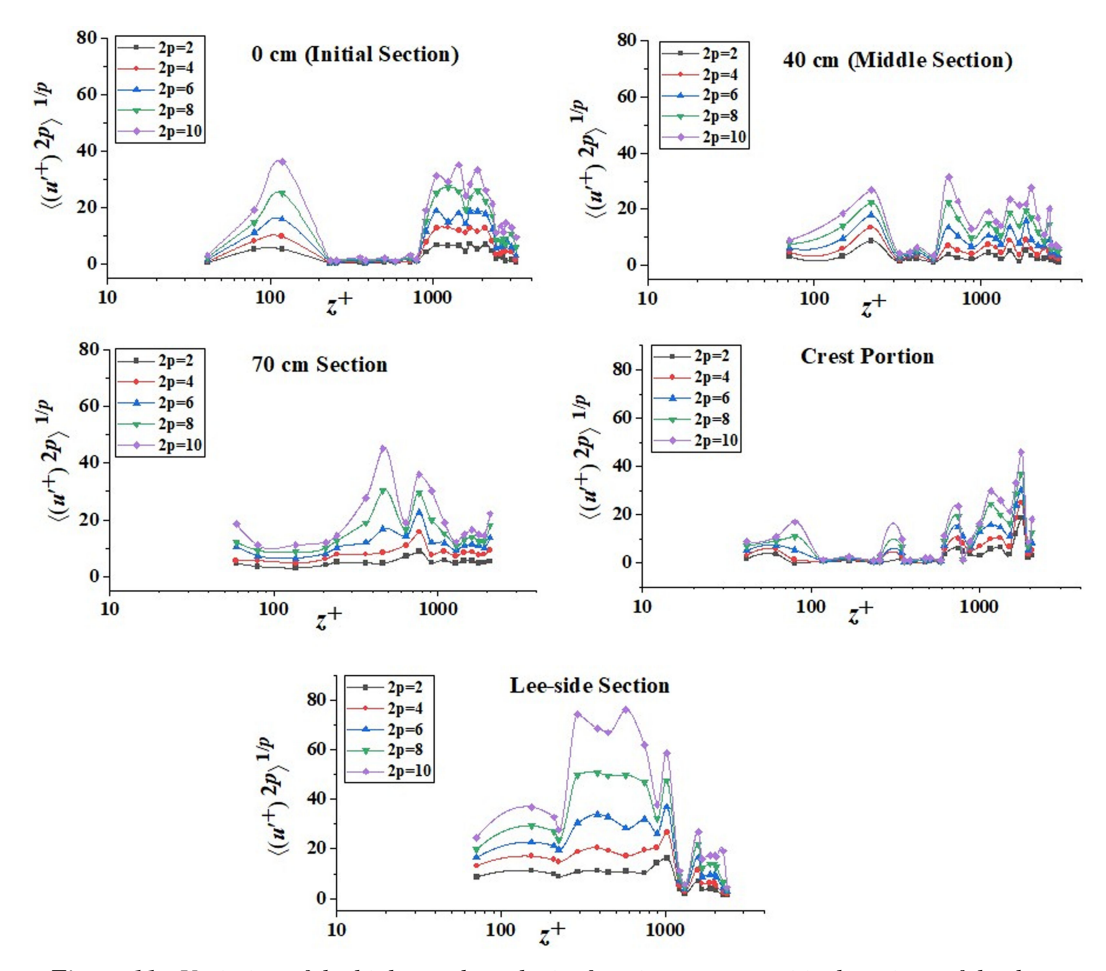


Figure 11. Variation of the higher-order velocity function at some critical sections of the dune.

The crest portion exhibits the highest structure function values, but is only confined towards the surface of the flow. On the lee-side section, the structure–function patterns exhibit the highest value, particularly in the wake region, confirming vortex shedding and maximum energy dissipation, generating complex and fluctuating turbulent behaviour in this region due to the development of scour holes. The sharp peaks in the structure–function curves at the lee-side section suggest the presence of intense turbulent bursts and strong nonlinear interactions. Thus, the structure–function analysis across the dune highlights a progression in turbulence intensity and intermittency in all the sections on the stoss side of the dune and redistribution on the lee side. These findings suggest the strong influence of bedform topography on turbulent flow structure, highlighting the importance of spatially resolved turbulence measurements in understanding sediment transport and flow dynamics over mobile beds.

# 3.7. Morphological patterns of the mobile bedforms

In addition to the experimental assessment of turbulence characteristics over mobile bedforms, the study also examines the morphological evolution of the bedform shape. Bedform morphology along the dune length was analysed using URS (ultrasonic ranging system). Four morphological profiles of the bedform surface were recorded at 8-hour intervals. Figure 12 illustrates how the change in bedform morphology changes with time.

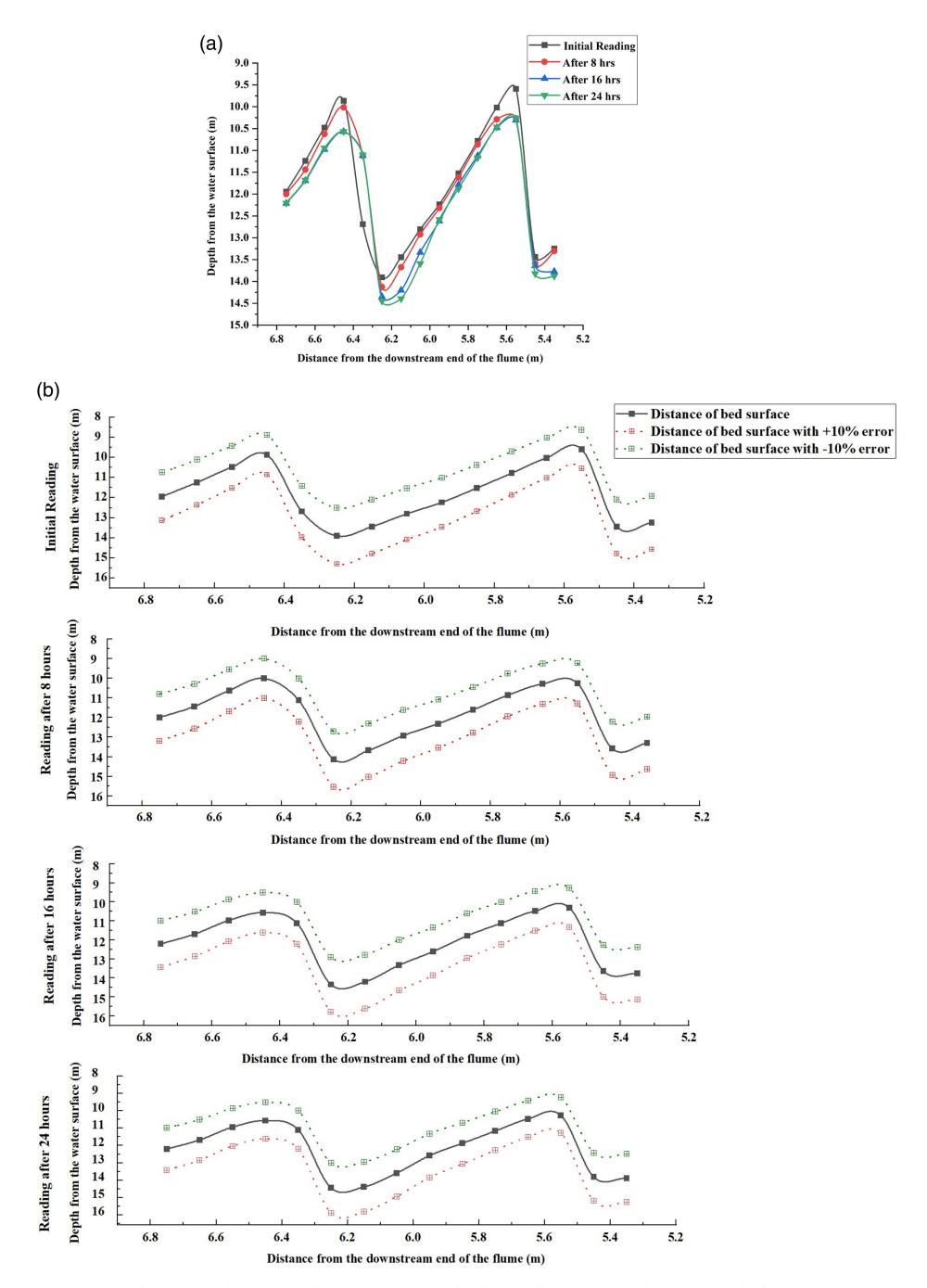


Figure 12. (a) Change in bedform morphology changes with time and (b) error plot.

The findings indicate a progressive increase in the maximum scour depth at the lee side of the dune. Initially, the depth from the water surface was 13 cm, gradually increasing to 13.5, 14.5 cm and eventually 14.8 cm over the observation period. Similarly, due to sediment being eroded from the crest region and transported downstream, the dune's crest migrated, increasing the distance from the water surface. Initial readings suggest the distance of the dune crest from the water surface to be below 9.5 cm, which increased to 10 cm at 8 h and approximately 10.8 cm at 24 h. This crest movement contributes to developing more sinuous, three-dimensional bedform features with time. Sediment transport in the river system with dunes primarily occurs due to sediment motion from the stoss side (upstream face) of the dune and

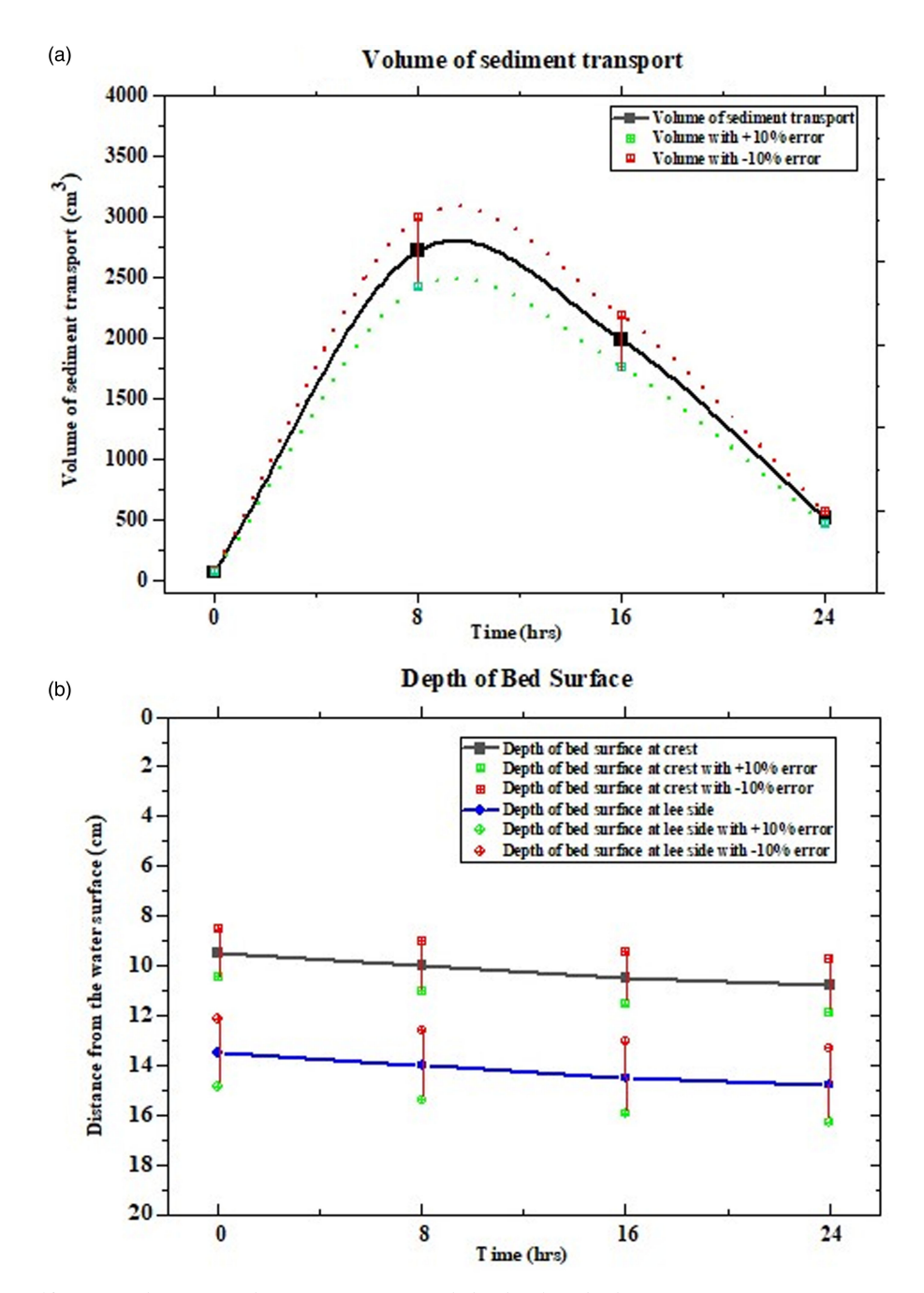


Figure 13. (a) Volume of sediment transport and (b) depth of bed surface from water surface over the experimental run.

the development of scour holes on the lee side, facilitating dune migration in the direction of the flow. Figure 13 depicts the change in depth of crest and scour, along with the volume of sediment transport over the experimental run.

During the first 8 hours, sediment transport was notably high, reaching ~2722 cm<sup>3</sup>. However, after the 16-h mark, the volume of sediment transport decreased to 1986 cm<sup>3</sup>. At the end of 24 hours, the transported sediment volume further reduced to 521 cm<sup>3</sup>, suggesting that the dune bedform was approaching

an equilibrium state, beyond which significant sediment motion would likely cease with time. The experimental results highlight a clear trend of increasing scour depth and crest elevation with time, pointing to active morphological evolution of the mobile bedform. The sediment transport volumes observed suggest that the dune undergoes an initial phase of high mobility, which diminishes over time as the system approaches equilibrium.

At the 24-h observation period, the amount of sediment transported was estimated to be  $\sim 521~\rm cm^3$ , highlighting that the dune bedform is on the verge of achieving equilibrium conditions. The results obtained from estimating the amount of sediment transport indicate that downward seepage significantly enhances sediment transport. As the downward seepage rate increases, the cumulative amount of sediment transported also increases, leading to a higher speed of bedform migration.

### 4. Discussions

The present experimental study provides a detailed description of the hydrodynamic processes and morphological evolution of mobile dune-shaped bedforms. The study underlines the interplay between velocity structure, turbulence and sediment transport, revealing the mechanisms responsible for dune migration and stability. While previous literature focused on analysing the flow dynamics over fixed bedform, they thus failed to directly couple turbulence statistics with the morphological evolution of mobile dunes. The profiles of streamwise velocity indicate a strong spatial variability across different dune sections. Negative velocities prevail in the near-bed region of the initial sections, confirming the presence of recirculation due to the wake generated by the preceding dune. Accelerated flow on the stoss side enhances flow shear, while the crest portion shows maximum streamwise velocity. The lee side of the dune is characterised by flow separation and reattachment, leading to a wake zone of reduced velocity but persistent near-bed turbulence. Similar observations were also reported in previous studies. These observations demonstrate how dunes generate alternate zones of accelerated and decelerated zones that promote variable amounts of sediment entrainment at different sections of the dune. The higher magnitude of Reynolds shear stress in the near-bed region at the initial and lee-side sections of the dune confirms vigorous turbulent mixing and enhanced sediment entrainment capacity. However, a lower magnitude of RSS values at the crest portion of the dune suggests limited entrainment and potential stabilisation. Results highlight the dominance of the streamwise component at the lee side of the dune, intensifying the development of scour holes and strengthening vortical structures.

Analysis of p.d.f.s shows that experimental data exhibit significant deviations at critical dune sections compared with the general trend of theoretical Gaussian-type assumptions. The streamwise velocity p.d.f.s show right-skewness on the stoss side and crest, indicative of asymmetric and intermittent bursts, whereas at the lee-side section of the dune, p.d.f.s are more symmetric, consistent with vortex-dominated wake flows. At the initial section, p.d.f.s of lateral functions agree with the theoretical distribution, but the deviations increase over the crest, reflecting the development of lateral eddies. The lee-side section again exhibits a symmetry trend, confirming reattachment and stabilisation. However, vertical velocity p.d.f.s reveal broad tails at the initial and lee-side sections, underscoring vortex shedding and chaotic vertical bursts that lift particles. The p.d.f.s deviate most at the crest portion as compared with the theoretical distribution pattern, reflecting maximum turbulence complexity in the crest region due to the influence of the wake generated at the lee-side section of the considered dune. P.d.f.s of Reynolds shear stress exhibit asymmetry and wide scatter, particularly at the lee side, showing the presence of strong, anisotropic turbulence structures. JSD quantifies and justifies these findings, confirming that the middle sections exhibit lower divergence (stabilised turbulence), while crest and lee sections show elevated divergence due to flow separation and intermittent bursts.

The results obtained from octant analysis suggest the dominance of sweep and ejection events at the initial, crest portion and lee-side section of the dune. Higher occurrence probability of a sweep event in the near-bed region of the initial sections, crest portion and lee-side section of the dune suggests enhanced sediment motion from these regions as compared with the middle section. The intensified sediment motion from the lee-side sections promotes continuous erosion and scour development, while sediment transport originating from the crest contributes to the overall downstream migration of the

bedform. The findings of the octant analysis also hold direct significance for explaining vortex shedding and the dominance of specific coherent structures. The alternation between ejections (upward movement of low-momentum fluid) and sweeps (downward penetration of high-momentum fluid) provides the necessary conditions for the formation of coherent vortices in the wake zone.

The spatial concentration of these events near the dune crest is consistent with the onset of vortex shedding, as the instability of the separated shear layer amplifies these burst-dominated motions. Hence, the findings also closely aligned with the observed non-Gaussian features of p.d.f.s, where the initial sections and the crest portion show heavy-tailed distributions due to the intermittent and intense occurrence of ejection and sweep events, which directly correspond to the generation of coherent vortices. The combined action of the dominating event (sweeps and ejections) would establish a cycle of sediment pickup, suspension and downstream delivery, which is further modulated by the coherent vortices shed in the wake of the dune crest. This coupling between turbulent structures and sediment movement explains the spatial variability in bedform evolution and highlights the role of bursting events as fundamental drivers of sediment dynamics in alluvial streams.

Structure function analysis highlights the intermittent and multi-scale nature of turbulence over the dune. Increasing magnitudes of structure function with higher orders confirm the dominance of extreme turbulent events in the near-bed region at the stoss side and in the wake region at the lee side of the dune. The crest exhibits enhanced intermittency near the surface, while the lee side displays the strongest turbulent bursts, confirming the role of vortex shedding in driving sediment suspension and energy dissipation. Results of morphological evolution of the dune highlight that the dune undergoes continuous evolution, with progressive scour deepening on the lee side and crest migration downstream. Sediment transport rates are high at the initial phase of experiments (up to 8 hours) but reduce substantially with time, indicating a transition towards equilibrium. The observed patterns confirm that dunes experience an initial adjustment phase leading to intense sediment motion, which is followed by stabilisation as the bedform reaches dynamic equilibrium with the flow.

The combined outcomes of the present mobile bed experimental study illustrate a unified mechanism governed by turbulence statistics in sediment transport. Alternating zones of high and low velocity along the dune length were identified, which correspond to peaks in Reynolds shear stress, turbulence intensities and coherent structures identified by octant analysis. Statistical analysis reveals the deviations from Gaussian behaviour coincide with these zones, highlighting the role of intermittent bursts in driving sediment motion. Further, structure functions confirm the scale-dependent and intermittent nature of turbulence near the bed, consistent with the observed morphological changes. Together, these findings confirm the presence of heterogeneous turbulence along the mobile dunes-shaped bedform, which generates alternating regions of sediment entrainment and deposition, with coherent structures acting as the primary drivers of sediment transport. The convergence of independent analytical approaches reinforces the robustness of this interpretation, providing a comprehensive perspective on how turbulence shapes mobile bedform evolution in alluvial channels.

### 5. Conclusions

The present study advances understanding of how turbulent flow structures govern the evolution of mobile dune bedforms in alluvial channels. Rather than treating turbulence statistics and morphology separately, the findings of the study demonstrate their coupled dynamics and reveal the key insights by linking these turbulence statistics directly to bedform morphological evolution, as follows.

Flow acceleration over the stoss side and deceleration with flow separation at the crest and lee side
generated strong spatial heterogeneity in turbulence intensity and Reynolds shear stress development of complex turbulence structures along the dune. These variations directly controlled
zones of sediment entrainment, scour formation and deposition at different sections of the dune.

- A higher magnitude of RSS and streamwise turbulence intensity in the near-bed region at both the
  initial and lee-side sections of the dune indicates zones of active sediment entrainment and transport. In contrast, reduced RSS near the crest suggests limited sediment mobilisation, although
  localised erosion can reshape the bedform.
- The patterns of turbulence intensities and Reynolds shear stresses confirm that streamwise turbulence is the primary driver of sediment entrainment, while lateral and vertical turbulence contribute to redistribution and suspension.
- The prevalence of sweep and ejection events, along with vortex shedding at the lee side, established a clear mechanistic link between bursting phenomena and sediment mobilisation. This coupling explains the observed scour-hole deepening and downstream dune migration, highlighting their fundamental role in shaping alluvial stream morphology
- P.d.f.s and higher-order structure functions exhibited clear deviations from Gaussian distributions, particularly at the initial and lee-side sections, revealing the intermittent, anisotropic and non-Gaussian nature of turbulence developed over dunes. These statistical signatures directly corresponded to the most dynamically active zones of erosion. The strongest intermittent events occurred at the lee-side section of the dune, making it the most dynamically active region for sediment erosion.
- Bedform morphology evolves dynamically over the 24-hour observation period, characterised
  by an increase in scour depth and migration of the crest in the downstream direction. However,
  the findings suggest that the sediment transport diminishes over time, highlighting the natural
  tendency of the system towards stability.

Thus, this study demonstrates that well-established turbulence tools, when applied to evolving dune-shaped bedforms, can yield new physical insights into how coherent flow structures drive sediment entrainment, scour development and dune migration. These findings can contribute to a more mechanistic understanding of turbulence—morphology interactions in alluvial channels, with implications for sediment management and river engineering. Further research can be extended to larger-scale dunes with variable sediment sizes and flow discharges to better represent natural riverine conditions. Coupling the present experimental results with high-resolution numerical simulations can also be done to improve predictive accuracy, which can have direct applications in flood management, navigation channel design and habitat preservation in alluvial rivers.

### **Notations**

h

z epun er une new
Vertical distance from the bedform surface
Median diameter of the particle
Instantaneous velocity in the direction of flow
Number of samples
Shields parameter
Critical Shields parameter
Shear velocity
Turbulent intensities of flow in streamwise, spanwise and vertical directions, respectively.
Fluctuating components associated with the flow in streamwise, spanwise and vertical directions, respectively
Occurrence probability of each event
Number of events in each class
Total number of bursting events

Depth of the flow

P(x) Probability distribution functions (p	p.d.f.s)
--	----------

 $P_u$ ,  $P_v$  and  $P_w$  P.d.f. of streamwise, spanwise and vertical velocity fluctuations, respectively

 $P_{\tau}$  P.d.f. of RSS

u(x) Velocity at position x

 $\delta_u(r)$  Velocity increment over distance r

 $S_n(r)$  nth-order structure function

**Author contribution.** P.B. did the experiments, analysed the observations and wrote the initial draft of the manuscript. V.D. analysed the observations and wrote the initial draft of the manuscript with P.B. B.K. conceptualised the idea and supervised the work. All authors wrote the final draft of the manuscript.

**Data availability statement.** The datasets used and analysed during the current study are available from the corresponding author upon reasonable request.

Funding statement. This research received no external funding.

Competing interests. The authors declare no conflicts of interest.

### References

- Anselmet, F., Gagne, Y., Hopfinger, E. J., & Antonia, R. A. (1984). High-order velocity structure functions in turbulent shear flows. *Journal of Fluid Mechanics*, 140, 63–89.
- Antonia, R. A., Zhu, Y., & Sokolov, M. (1995). Effect of concentrated wall suction on a turbulent boundary layer. *Physics of Fluids*, 7(10), 2465–2474.
- ASCE Task Committee on Flow and Transport over Dunes (2002). Flow and transport over dunes. *Journal of Hydraulic Engineering*, 128(8), 726–728.
- Bauri, K. P., Sarkar, A., & Nones, M. (2024). Three-dimensional bursting process and turbulent coherent structure within scour holes at various development stages around a cylindrical structure. *Journal of Fluid Mechanics*, 997, A61.
- Behera, P. K., Deshpande, V., & Kumar, B. Morphodynamics of mobile dunes under seeping environment. *Physics of Fluids*, *AIP*, *37*, 026621.
- Behera, P. K., Patel, M., Deshpande, V., & Kumar, B. (2024). Patterns of turbulent flow structures over dune-shaped bed features under the influence of downward seepage. *Experimental Thermal and Fluid Science*, 153, 111128.
- Benzi, R., Biferale, L., Ciliberto, S., Struglia, M. V., & Tripiccione, R. (1996). Generalized scaling in fully developed turbulence. *Physica D: Nonlinear Phenomena*, 96(1-4), 162–181.
- Bernard, P. S., & Handler, R. A. (1990). Reynolds stress and the physics of turbulent momentum transport. *Journal of Fluid Mechanics*, 220, 99–124.
- Best, J. I. M. (1992). On the entrainment of sediment and initiation of bed defects: Insights from recent developments within turbulent boundary layer research. *Sedimentology*, 39(5), 797–811.
- Best, J. (2005). The fluid dynamics of river dunes: A review and some future research directions. *Journal of Geophysical Research:* Earth Surface, 110(F4).
- Best, J. L., Ashworth, P. J., Bristow, C. S., & Roden, J. (2003). Three-dimensional sedimentary architecture of a large, mid-channel sand braid bar, Jamuna River, Bangladesh. *Journal of Sedimentary Research*, 73(4), 516–530.
- Bridge, J. S. (2003). Rivers and floodplains: Forms, processes, and sedimentary record. John Wiley & Sons.
- Carling, P. A., Richardson, K., & Ikeda, H. (2005). A flume experiment on the development of subaqueous fine-gravel dunes from a lower-stage plane bed. *Journal of Geophysical Research: Earth Surface*, 110(F4).
- Cellino, M., & Graf, W. H. (2000). Experiments on suspension flow in open channels with bedforms. *Journal of Hydraulic Research*, 38(4), 289–298.
- Das, D., Ganti, V., & Reesink, A. (2024). The role of fluvial morphodynamic hierarchy in shaping bedform deposits. *Geophysical Research Letters*, 51(20), e2024GL110678.
- Deshpande, V., & Kumar, B. (2016). Turbulent flow structures in alluvial channels with curved cross-sections under conditions of downward seepage. *Earth Surface Processes and Landforms*, 41(8), 1073–1087.
- Dimas, A. A., Fourniotis, N. T., Vouros, A. P., & Demetracopoulos, A. C. (2008). Effect of bed dunes on spatial development of open-channel flow. *Journal of Hydraulic Research*, 46(6), 802–813.
- Einstein, H. A. (1950). The bed-load function for sediment transportation in open channel flows (No. 1026). US Department of Agriculture.
- Frisch, U., & Kolmogorov, A. N. (1995). Turbulence: The legacy of AN Kolmogorov. Cambridge University Press.

- Goring, D. G., & Nikora, V. I. (2002). Despiking acoustic Doppler Velocimeter data. *Journal of Hydraulic Engineering*, 128(1), 117–126.
- Grass, A. J. (1971). Structural features of turbulent flow over smooth and rough boundaries. Journal of Fluid Mechanics, 50(2), 233–255.
- Gurugubelli, Y., Timbadiya, P. V., & Barman, B. (2025). Probability density functions in an asymmetric alluvial sinuous channel. In *Stochastic environmental research and risk assessment* (pp. 1–19).
- Huai, W., Yang, L., & Guo, Y. (2020). Analytical solution of suspended sediment concentration profile: Relevance of dispersive flow term in vegetated channels. Water Resources Research, 56(7), e2019WR027012.
- Huai, W. X., Zhang, J., Katul, G. G., Cheng, Y. G., Tang, X., & Wang, W. J. (2019). The structure of turbulent flow through submerged flexible vegetation. *Journal of Hydrodynamics*, 31(2), 274–292.
- Ikani, N., Pu, J. H., Taha, T., Hanmaiahgarib, P. R., & Penna, N. (2023). Bursting phenomenon created by bridge piers group in open channel flow. Environmental Fluid Mechanics, 23(1), 125–140.
- Järvelä, J. (2005). Effect of submerged flexible vegetation on flow structure and resistance. *Journal of Hydrology*, 307(1–4), 233–241.
- Keshavarzi, A. R., & Gheisi, A. R. (2006). Stochastic nature of three dimensional bursting events and sediment entrainment in vortex chamber. Stochastic Environmental Research and Risk Assessment, 21(1), 75–87.
- Kleinhans, M. G. (2001). The key role of fluvial dunes in transport and deposition of sand-gravel mixtures, a preliminary note. *Sedimentary Geology*, 143(1–2), 7–13.
- Kleinhans, M. G. (2002). Sorting out sand and gravel: sediment transport and deposition in sand-gravel bed rivers. Netherlands Geographical Studies, 293 (Ph.D. Thesis, Royal Dutch Geographical Society/Utrecht University, p. 317). ISBN 90-6809-328-2.
- Li, Y., Zhang, F., Li, Z., & Yang, X. (2024). Impacts of inflow turbulence on the flow past a permeable disk. *Journal of Fluid Mechanics*, 999, A30.
- Lu, S. S., & Willmarth, W. W. (1973). Measurements of the structure of the Reynolds stress in a turbulent boundary layer. *Journal of Fluid Mechanics*, 60(3), 481–511.
- Lyn, D. A., & Altinakar, M. (2002). St. Venant-Exner equations for near-critical and Transcritical flows. *Journal of Hydraulic Engineering*, 128(6), 579–587.
- Mahon, R. C., Ganti, V., Kelley, M. M., Das, D., Sanchez, V., & Portocarrero, G. (2024). Lower bound on preserved flood duration in fluvial bedform stratigraphy. *Geophysical Research Letters*, 51(15), e2024GL109622.
- Marsh, N. A., Western, A. W., & Grayson, R. B. (2004). Comparison of methods for predicting incipient motion for sand beds. *Journal of Hydraulic Engineering*, 130(7), 616–621.
- Marusic, I., Monty, J. P., Hultmark, M., & Smits, A. J. (2013). On the logarithmic region in wall turbulence. *Journal of Fluid Mechanics*, 716, R3.
- McLean, S. R., Nelson, J. M., & Wolfe, S. R. (1994). Turbulence structure over two-dimensional bed forms: Implications for sediment transport. *Journal of Geophysical Research: Oceans*, 99(C6), 12729–12747.
- Mishra, R. K., Barman, B., & Pathania, T. (2024). Three-dimensional modeling of hydro-morphodynamic characteristics of mining affected alluvial channel using TELEMAC and GAIA. *Physics of Fluids*, 36(10).
- Nakagawa, H., & Nezu, I. (1977). Prediction of the contributions to the Reynolds stress from bursting events in open-channel flows. *Journal of Fluid Mechanics*, 80(1), 99–128.
- Nezu, I. (1977). Turbulent structure in open-channel flows. Kyoto University.
- Nezu, I., Tominaga, A., & Nakagawa, H. (1993). Field measurements of secondary currents in straight rivers. *Journal of Hydraulic Engineering*, 119(5), 598–614.
- Parisi, G., & Frisch, U. (1985). A multifractal model of intermittency. In Turbulence and predictability in geophysical fluid dynamics and climate dynamics (pp. 84–88).
- Pathikonda, G., & Christensen, K. T. (2017). Inner-outer interactions in a turbulent boundary layer overlying complex roughness. Physical Review Fluids, 2(4), 044603.
- Raudkivi, A. J. (1997). Ripples on the stream bed. Journal of Hydraulic Engineering, 123(1), 58-64.
- Raudkivi, A. J., & Witte, H. H. (1990). Development of bed features. Journal of Hydraulic Engineering, 116(9), 1063–1079.
- Raupach, M. (1981). Conditional statistics of Reynolds stress in rough-wall and smooth-wall turbulent boundary layers. *Journal of Fluid Mechanics*, 108, 363–382.
- Robert, A., & Uhlman, W. (2001). An experimental study on the ripple-dune transition. Earth Surface Processes and Landforms: The Journal of the British Geomorphological Research Group, 26(6), 615–629.
- Sharma, A., & Kumar, B. (2016). Probability distribution functions of turbulence in seepage-affected alluvial channel. Fluid Dynamics Research, 49(1), 015508.
- Shvidchenko, A. B., & Pender, G. (2001). Macroturbulent structure of open-channel flow over gravel beds. *Water Resources Research*, 37(3), 709–719.
- Sreenivasan, K. R., Sahay, A., & Panton, R. (1997). Self-sustaining mechanisms of wall turbulence (pp. 253–272). Computational Mechanics Publication.
- Taye, J., & Kumar, B. 2021, Experimental study on near-bed flow turbulence of sinuous channel with downward seepage. InProceedings of the Institution of Civil Engineers-Water Management (Vol. 174, pp. 173–186). Thomas Telford Ltd.
- Tayfur, G., & Singh, V. P. (2006). Kinematic wave model of bed profiles in alluvial channels. Water Resources Research, 42(6).

- Tayfur, G., & Singh, V. P. (2007). Kinematic wave model for transient bed profiles in alluvial channels under nonequilibrium conditions. *Water Resources Research*, 43(12).
- Van Rijn, L. C. (1984). Sediment transport, part I: Bed load transport. Journal of Hydraulic Engineering, 110(10), 1431–1456.
- Venditti, J. G., Church, M., & Bennett, S. J. (2005). Morphodynamics of small-scale superimposed sand waves over migrating dune bed forms. Water resources research, 41(10).
- Wang, X., Gualtieri, C., & Huai, W. (2023). Grain shear stress and bed-load transport in open channel flow with emergent vegetation. *Journal of Hydrology*, 618, 129204.
- Xie, Z., Lin, B., & Falconer, R. A. (2014). Turbulence characteristics in free-surface flow over two-dimensional dunes. *Journal of Hydro-Environment Research*, 8(3), 200–209.
- Yang, W., & Choi, S. U. (2009). Impact of stem flexibility on mean flow and turbulence structure in depth-limited open channel flows with submerged vegetation. *Journal of Hydraulic Research*, 47(4), 445–454.
- Yue, W., Lin, C. L., & Patel, V. C. (2006). Large-eddy simulation of turbulent flow over a fixed two-dimensional dune. *Journal of Hydraulic Engineering*, 132(7), 643–651.
- Zomer, J. Y., & Hoitink, A. J. F. (2024). Evidence of secondary bedform controls on river dune migration. Geophysical Research Letters, 51(15), e2024GL109320.

Cite this article: Behera PK, Deshpande V and Kumar B (2025). Dynamics of turbulent flow over mobile dune. *Flow*, 5, E41. https://doi.org/10.1017/flo.2025.10035